JOC Featured Article

Formation of Supramolecular Polymers and Discrete Dimers of Perylene Bisimide Dyes Based on Melamine−Cyanurates Hydrogen-Bonding Interactions

Tomohiro Seki,[†] Shiki Yagai,*[,†,‡] Takashi Karatsu,[†] and Akihide Kitamura[†]

Department of Applied Chemistry and Biotechnology, Graduate School of Engineering, Chiba University, Yayoi-cho, Inage-ku, Chiba 263-8522, Japan, and PRESTO, Japan Science and Technology Agency (JST), 4-1-8 Honcho Kawaguchi, Saitama, Japan

yagai@faculty.chiba-u.jp

Received February 9, 2008

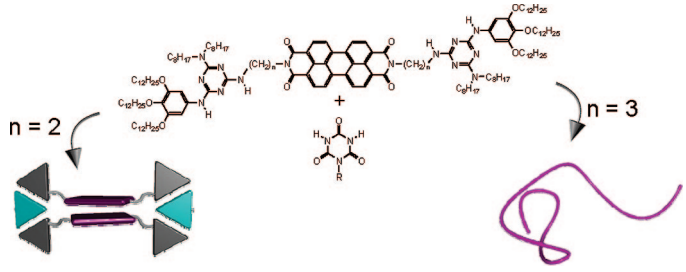

Melamine-linked perylene bisimide dyes (MPBIs) bearing an ethylene or trimethylene group as linker moieties were synthesized, and their self-aggregation and coaggregation with cyanurates through complementary triple hydrogen bonds have been investigated. UV/vis studies revealed that both the MPBIs self-assemble in nonpolar organic solvent through $\pi-\pi$ stacking interaction between perylene cores, giving self-aggregates with nearly identical thermal stabilities. Upon addition of 1 equiv of cyanurate components, however, the stabilities of the resulting aggregates were dramatically changed between the two systems, suggesting the formation of different types of hydrogen-bonded supramolecular species. Dynamic light scattering and atomic force microscopic studies revealed that the system featuring ethylene linker moieties generates a discrete dimer of MPBI supported by two cyanurate molecules, whereas the system featuring trimethylene linker moieties affords extended supramolecular polymers hierarchically organizing into nanoscopic fibers. These results demonstrate that it is possible to obtain distinct supramolecular species by just changing the number of carbon atoms at the linker moieties of MPBI components. The present strategy for the fabrication of discrete or polymeric supramolecular assemblies should be applicable to other functional π-conjugated molecules.

Introduction

Construction of self-assemblies of π-conjugated molecules with controlled size, shape, and overall morphologies is a topic of current interest as the bottom-up approach toward organic optoelectronic devices.[1−4] While one-dimensional polymeric assemblies of π-conjugated molecules often self-organize into fibrous nanostructures that are promising as conducting organic nanowires,[5] discrete supramolecular species soluble in organic solvent can be used as processable functional materials showing optical and electronic properties distinct from those of monomeric molecules.

Among various functional π-conjugated molecules, perylene bisimide (PBI) dyes have attracted considerable attention because of their outstanding photophysical properties in addition

[†] Chiba University.
[‡] PRESTO, JST.

(1) *Supramolecular Dye Chemistry*; Würthner, F. Ed.; Topics in Current Chemistry 258; Springer-Verlag: Heidelberg, 2005.
(2) Hoeben, F. J. M.; Jonkheijm, P.; Meijer, E. W.; Schenning, A. P. H. J. *Chem. Rev.* **2005**, *105*, 1491–1546.
(3) Schenning, A. P. H. J.; Meijer, E. W. *Chem. Commun.* **2005**, 3245–3258.
(4) Ajayaghosh, A.; Praveen, V. K. *Acc. Chem. Res.* **2007**, *40*, 644–656.
(5) Schenning, A. P. H. J.; Jonkheijm, P.; Hoeben, F. J. M.; Van Herrikhuyzen, J.; Meskers, S. C. J.; Meijer, E. W.; Herz, L. M.; Daniel, C.; Silva, C.; Phillips, R. T.; Friend, R. H.; Beljonne, D.; Miura, A.; De Feyter, S.; Zdanowska, M.; Uji-I, H.; De Schryver, F. C.; Chen, Z.; Würthner, F.; Mas-Torrent, M.; Den Boer, D.; Durkut, M.; Hadley, P. *Synth. Met.* **2004**, *147*, 43–48.

10.1021/jo800338f CCC: $40.75
Published on Web 04/08/2008

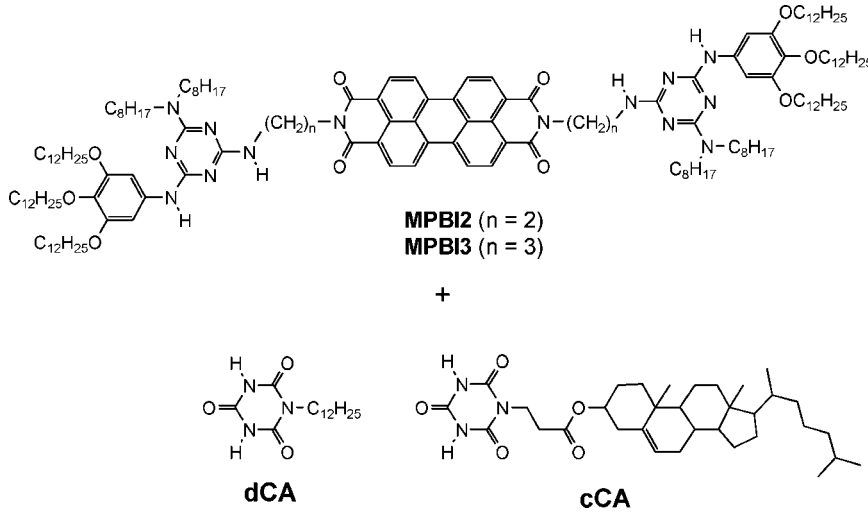

FIGURE 1. Structures of melamine-linked perylene bisimides **MPBI2** and **MPBI3** and cyanurates **dCA** and **cCA**.

to their versatility as supramolecular building blocks.[6–10] Combination of their strong $\pi-\pi$ stacking properties with other noncovalent interactions such as hydrogen bonds, coordination bonds, and solvophobic interactions allows diverse supramolecular assemblies such as one-dimensional nanofibers,[11–18] vesicles,[19] and discrete cyclic oligomers.[20–23] Recently, we have also contributed to the facile preparation of crystalline nanofibers consisting of perylene bisimides based on the triple-hydrogen-bond-directed supramolecular copolymerization of melamine-linked perylene bisimide (MPBI) and a cyanurate (see Figure 1 for general structures).[24,25] One of the appealing points in our system is that overall morphologies of supramolecular nanofibers might be regulated just by changing the complimentary components (i.e., cyanurates/barbiturates).[26–28] Another appealing point is that supramolecular structures of hydrogen-bonded species formed at the lowest level of the organization hierarchy could be controlled by the length of alkyl linker moieties of building blocks, as demonstrated by our recent reports on the diversification of supramolecular merocyanine dye assemblies.[29,30]

Herein, we focused on the effect of the linker moieties of MPBI on supramolecular species formed upon complexation with cyanurates. The previously reported MPBI features trimethylene linkers, giving crystalline nanofibers upon complexation with dodecyl cyanurate (**dCA**, Figure 1) in methylcyclohexane (MCH).[24] In the present study, we prepared **MPBI2** and **MPBI3** where the perylene bisimide core and the melamine moieties are linked through the ethylene and trimethylene linkers, respectively. The tri(dodecyloxy)phenyl (TDP) group is newly introduced to melamine moieties, which makes the resulting supramolecular species soluble in nonpolar solvent and thereby facilitates the solution-state studies. Despite a marginal structural difference in the length of alkyl linkers, the aggregation of **MPBI2** and **MPBI3** with **dCA** generates remarkably distinct supramolecular species as revealed by various spectroscopic and microscopic observations.

Results

Synthesis. MPBI2 and **MPBI3** were prepared according to Scheme 1. Melamine derivatives **1** and **2** possessing TDP and an ω-aminoalkyl group were prepared as hydrogen-bonding moieties. Imidization of 3,4:9,10-tetracarboxylic dianhydride with **1** and **2** was carried out in imidazole under refluxing, affording **MPBI2** and **MPBI3**, respectively. These MPBI compounds are highly soluble in common organic solvents and purified readily by using silica gel chromatography.

(6) Langhals, H. *Helv. Chim. Acta* **2005**, *88*, 1309–1343.
(7) Würthner, F. *Chem. Commun.* **2004**, 1564–1579.
(8) Elemans, J. A. A. W.; van Hameren, R.; Nolte, R. J. M.; Rowan, A. E. *Adv. Mater.* **2006**, *18*, 1251–1266.
(9) Grimsdale, A. C.; Müllen, K. *Angew. Chem., Int. Ed.* **2005**, *44*, 5592–5629.
(10) Wasielewski, M. R. *J. Org. Chem.* **2006**, *71*, 5051–5066.
(11) Li, X.-Q.; Stepanenko, V.; Chen, Z.; Prins, P.; Siebbeles Laurens, D. A.; Würthner, F. *Chem. Commun.* **2006**, 3871–3873.
(12) Che, Y.; Datar, A.; Balakrishnan, K.; Zang, L. *J. Am. Chem. Soc.* **2007**, *129*, 7234–7235.
(13) Balakrishnan, K.; Datar, A.; Naddo, T.; Huang, J.; Oitker, R.; Yen, M.; Zhao, J.; Zang, L. *J. Am. Chem. Soc.* **2006**, *128*, 7390–7398.
(14) Balakrishnan, K.; Datar, A.; Oitker, R.; Chen, H.; Zuo, J.; Zang, L. *J. Am. Chem. Soc.* **2005**, *127*, 10496–10497.
(15) Yan, P.; Chowdhury, A.; Holman, M. W.; Adams, D. M. *J. Phys. Chem. B* **2005**, *109*, 724–730.
(16) Würthner, F.; Hanke, B.; Lysetska, M.; Lambright, G.; Harms, G. S. *Org. Lett.* **2005**, *7*, 967–970.
(17) Sugiyasu, K.; Fujita, N.; Shinkai, S. *Angew. Chem., Int. Ed.* **2004**, *43*, 1229–1233.
(18) Kaiser, T. E.; Wang, H.; Stepanenko, V.; Würthner, F. *Angew. Chem., Int. Ed.* **2007**, *46*, 5541–5544.
(19) Zhang, X.; Chen, Z.; Würthner, F. *J. Am. Chem. Soc.* **2007**, *129*, 4886–4887.
(20) Würthner, F.; You, C.-C.; Saha-Moller Chantu, R. *Chem. Soc. Rev* **2004**, *33*, 133–146.
(21) Sautter, A.; Kaletas, B. K.; Schmid, D. G.; Dobrawa, R.; Zimine, M.; Jung, G.; Van Stokkum, I. H. M.; De Cola, L.; Williams, R. M.; Würthner, F. *J. Am. Chem. Soc.* **2005**, *127*, 6719–6729.
(22) Würthner, F.; Sautter, A. *Chem. Commun.* **2000**, 445–446.
(23) Würthner, F.; Sautter, A.; Schmid, D.; Weber, P. J. A. *Chem.−Eur. J.* **2001**, *7*, 894–902.
(24) Yagai, S.; Monma, Y.; Kawauchi, N.; Karatsu, T.; Kitamura, A. *Org. Lett.* **2007**, *9*, 1137–1140.
(25) Perylene bisimide assemblies based on multiple hydrogen-bonding interactions: (a) Yagai, S. *J. Photochem. Photobiol. C: Photochem. Rev.* **2006**, *7*, 164–182. (b) Würthner, F.; Thalacker, C.; Sautter, A. *Adv. Mater.* **1999**, *11*, 754–758. (c) Würthner, F.; Thalacker, C.; Sautter, A.; Schartl, W.; Ibach, W.; Hollricher, O. *Chem.−Eur. J.* **2000**, *6*, 3871–3886. (d) Liu, Y.; Zhuang, J.; Liu, H.; Li, Y.; Lu, F.; Gan, H.; Jiu, T.; Wang, N.; He, X. ; Zhu, D. *ChemPhysChem.* **2004**, *5*, 1210–1215. (e) Sinks, L. E.; Rybtchinski, B.; Iimura, M.; Jones, B. A.; Goshe, A. J.; Zuo, X.; Tiede, D. M. ; Li, X.; Wasielewski, M. R. *Chem. Mater.* **2005**, *17*, 6295–6303. (f) Yagai, S.; Seki, T.; Karatsu, T.; Kitamura, A.; Würthner, F. *Angew Chem., Int. Ed.*, in press.
(26) Yagai, S.; Higashi, M.; Karatsu, T.; Kitamura, A. *Chem. Mater.* **2004**, *16*, 3582–3585.
(27) Yagai, S.; Higashi, M.; Karatsu, T.; Kitamura, A. *Chem. Mater.* **2005**, *17*, 4392–4398.
(28) Yagai, S.; Karatsu, T.; Kitamura, A. *Langmuir* **2005**, *21*, 11048–11052.
(29) Yagai, S.; Higashi, M.; Karatsu, T.; Kitamura, A. *Chem. Commun.* **2006**, 1500–1502.
(30) Yagai, S.; Kinoshita, T.; Higashi, M.; Kishikawa, K.; Nakanishi, T.; Karatsu, T.; Kitamura, A. *J. Am. Chem. Soc.* **2007**, *129*, 13277–13287.

SCHEME 1. Synthesis of MPBI2 and MPBI3[a]

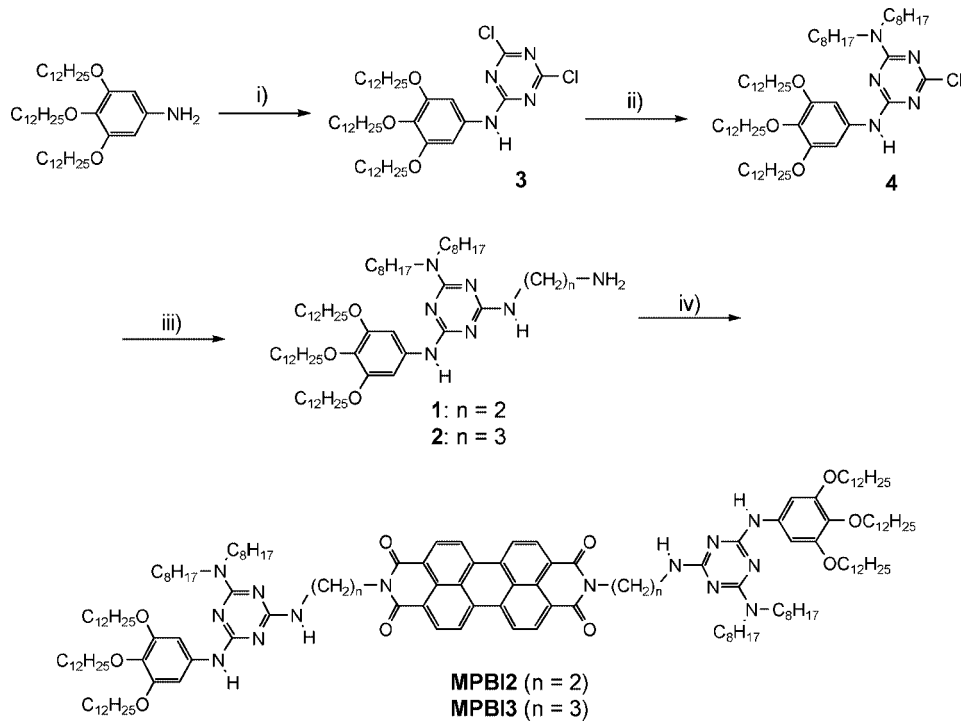

[a] (i) 1,3,5-trichloro-*s*-triazine, THF, rt, 2 h; (ii) dioctylamine, THF, rt, 2.5 h; (iii) 1,2-ethylenediamine (for **2**) or 1,3-propanediamine (for **3**), THF, 80 °C, overnight; (iv) perylene-3,4:9,10-tetracarboxylic dianhydride, zinc acetate, imidazole, 130 °C, 7 h−overnight.

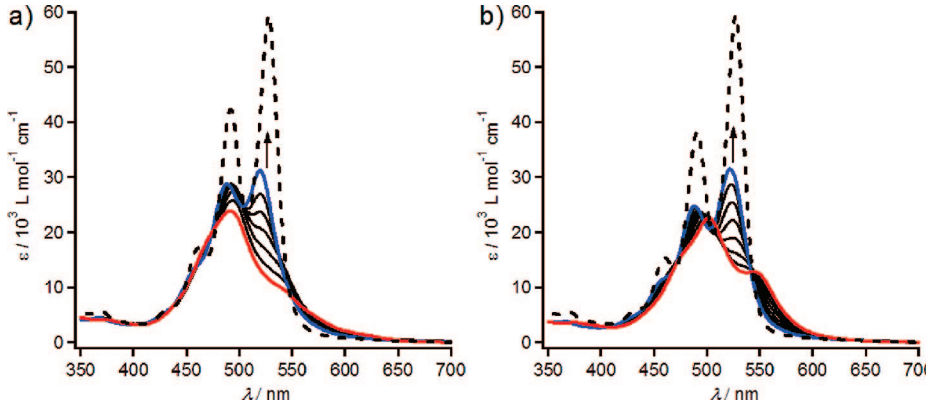

FIGURE 2. Temperature-dependent UV/vis spectra of (a) **MPBI2** and (b) **MPBI3** in MCH ($c = 1.4 \times 10^{-5}$ M). Temperature range: 20−90 °C. The spectra at 20 and 90 °C are drawn by red and blue lines, respectively. Arrows indicate changes upon increasing temperature. Dotted curves are the monomeric spectra recorded in CH_2Cl_2 at 25 °C.

UV/Vis Studies. Similar to other core-unsubstituted PBIs possessing aliphatic chains at the imide positions,[31] **MPBI2** and **MPBI3** in apolar solvents such as methylcyclohexane (MCH) show absorption spectra characteristic of $\pi-\pi$ stacked aggregates. Red curves in Figure 2 were the spectra recorded in MCH at a concentration of 1.4×10^{-5} M. Compared to those of the molecularly dissolved state in dichloromethane (dashed curves), the spectra in MCH are less structured due to strong electronic interaction between perylene cores. The stacking arrangement is most likely the H-type with rotational displacement along the stacking axis.[32] One may notice that **MPBI2** shows a less structured spectrum compared to that of **MPBI3**: a clear vibrational shoulder at $\lambda = 545$ nm observed for **MPBI3** is less pronounced for **MPBI2**. This suggests that the length of the alkyl linkers of MPBIs have some impact on the $\pi-\pi$ stacking arrangement of perylene cores. Since the number of carbon atoms at the linker moieties determines the orientation of the hydrogen-bonding melamine moieties, the observed effect of the linker length must be related to the presence of two-point or more nonspecific intermolecular hydrogen-bonding interactions between melamine moieties.[33,34]

Variable-temperature UV/vis measurements were carried out to compare the thermal stabilities of the self-aggregates (Figure 2). Both **MPBI2** and **MPBI3** showed thermal dissociation upon increasing temperature (from red to blue spectra). When the

(31) Würthner, F.; Thalacker, C.; Diele, S.; Tschierske, C. *Chem.−Eur. J.* **2001**, *7*, 2245–2253.
(32) Chen, Z.; Stepanenko, V.; Dehm, V.; Prins, P.; Siebbeles, L. D. A.; Seibt, J.; Marquetand, P.; Engel, V.; Würthner, F. *Chem.−Eur. J.* **2007**, *13*, 436–449.
(33) Thalacker, C.; Würthner, F. *Adv. Funct. Mater.* **2002**, *12*, 209–218.
(34) Jonkheijm, P.; Miura, A.; Zdanowska, M.; Hoeben, F. J. M.; De Feyter, S.; Schenning, A. P. H. J.; De Schryver, F. C.; Meijer, E. W. *Angew. Chem., Int. Ed.* **2004**, *43*, 74–78.

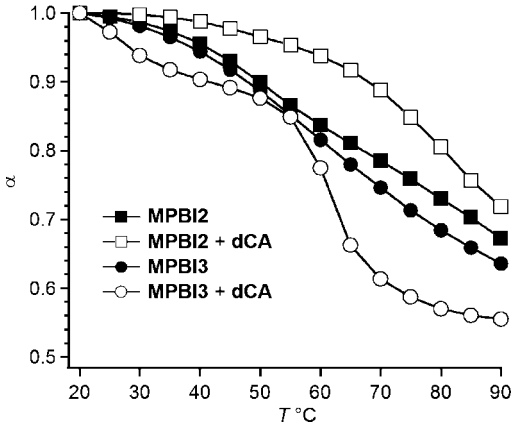

FIGURE 3. Plots of the fractions of aggregated molecules (α) against temperature for the temperature-dependent UV/vis spectra of **MPBI2** (■, Figure 2) and **MPBI3** (●, Figure 2) and **MPBI2·dCA** (□, Figure 5) and **MPBI3·dCA** (○, Figure 5). The fractions of aggregated species (α) are calculated from ϵ at around 527 nm according to the equation $(\epsilon_{monomer} - \epsilon)/(\epsilon_{monomer} - \epsilon_{aggregate})$, where $\epsilon_{aggregate}$ and $\epsilon_{monomer}$ were taken from fully aggregated spectra in MCH and completely monomeric spectra in CH_2Cl_2, respectively.

fractions of aggregated molecules (α) are plotted versus temperature, almost linear dissociation processes were revealed for both the systems (closed squares and circles in Figure 3). Though **MPBI2** showed slightly higher stability compared to **MPBI3**, the difference is very small, indicating that the self-aggregation is mainly driven by $\pi-\pi$ stacking interaction between perylene cores.

The effect of linker moieties of MPBIs is amplified upon aggregation with **dCA**. Figures 4a and b shows the UV/vis titration experiments of **MPBI2** and **MPBI3** with **dCA**, respectively. When **dCA** was titrated to the self-aggregated **MPBI2** and **MPBI3**, both the systems kept absorption properties characteristic of $\pi-\pi$ stacked perylene cores, indicating that the resulting hydrogen-bonded coaggregates also have $\pi-\pi$ stacked perylene cores. However, spectral transitions of the two systems induced by **dCA** are significantly different. For **MPBI2**, the addition of **dCA** rendered the spectra more structured with a hyperchromic effect, suggesting that the stacking arrangement of perylene cores becomes more uniform. In sharp contrast, **MPBI3** shows a hypochromic effect with the appearance of an additional hypsochromically shifted band at $\lambda_{max} = 470$ nm.[35] This spectral change demonstrates that the stacking arrangement of **MPBI3** becomes inhomogeneous upon aggregation with **dCA**. The spectral changes observed for both MPBIs leveled off at around **MPBI2/3**:**dCA** = 1:1 (Figure 4c), indicating the nearly quantitative aggregation of these modules through triple hydrogen bonding under diluted conditions.

The stabilities of **MPBI2·dCA** and **MPBI3·dCA** coaggregates were also compared by means of variable-temperature UV/vis measurements (Figure 5), and the fractions of aggregated molecules (α) are plotted versus temperature (open squares and circles in Figure 3). The nonlinear relationship between α and temperature in both the systems strongly suggests the cooperativity between hydrogen-bonding and $\pi-\pi$ stacking interactions. In contrast to the self-aggregates, the coaggregates showed thermal stabilities which are strongly dependent on the linker length. While **MPBI2** showed an increase in the stability upon complexation with **dCA**, **MPBI3** showed a decrease in the stability. Such a contrary effect of **dCA** is most likely related to the generation of different types of supramolecular species through triple hydrogen bonds. The higher stability of **MPBI2·dCA** is indicative of the formation of a discrete dimer held together by two **dCA** molecules through 12 hydrogen bonds in addition to $\pi-\pi$ stacking interaction between perylene cores (Figure 6). This was rationalized by a prominently structured absorption spectrum of **MPBI2·dCA** (red curve in Figure 5a) as compared to the spectra of **MPBI2**, **MPBI3**, and **MPBI3·dCA**, showing that the $\pi-\pi$ stacking arrangements of perylene cores are uniform. On the other hand, the supramolecular species of **MPBI3·dCA** proved to be polymeric by dynamic light scattering (DLS) and atomic force microscopic (AFM) studies as described in the following sections.

Dynamic Light Scattering Studies. The previously reported MPBI·**dCA** coaggregates were not suitable for our dynamic light scattering (DLS) instrument equipped with a He−Ne laser (632.8 nm) because the aggregated chromophores absorb the laser light and give rise to emission unfavorable for DLS analysis. However, the present MPBIs would be analyzed by our DLS instrument owing to the quantitative fluorescence quenching of perylene bisimide chromophores via the intramolecular electron transfer with the electron-rich tridodecyloxyphenyl groups.[31,25e]

First, we studied self-aggregates of **MPBI2** and **MPBI3** in MCH at concentrations ranging from 1.4×10^{-5} to 5×10^{-3} M. However, no large aggregates were detected from these solutions, indicating that self-aggregates are exchanging rapidly with monomer on the time scale of DLS (ms). By contrast, DLS of **MPBI2·dCA** and **MPBI3·dCA** coaggregates in MCH showed the formation of well-defined aggregated species. For **MPBI3·dCA**, large aggregated species with an average hydrodynamic diameter of 250 nm were detected for a freshly prepared solution with a concentration of 5×10^{-4} M (closed circles in Figure 7). After several hours, however, hydrodynamic diameters of the aggregates exceed 1000 nm, and eventually filamentous precipitates were visible by the naked eye. These results demonstrate the formation of extended supramolecular polymers from **MPBI3·dCA**.[36–38]

On the contrary, **MPBI2·dCA** does not show any detectable aggregates at micromolar concentration regime, indicating the absence of large polymeric species. Upon increasing the concentration up to 1×10^{-3} M, however, a monodisperse aggregate 8.4 nm in hydrodynamic diameter starts to be detected reproducibly (open circles in Figure 7). The aggregate was stable for more than a week, and its hydrodynamic diameter did not change upon increasing the concentration up to 5×10^{-3} M. These observations confirm the formation of a stable discrete aggregate. Considering the accuracy of dynamic light scattering of small aggregate species, the observed hydrodynamic diameter is in good agreement with the gyration diameter of the molecular modeled discrete dimer (6.9 nm, Figure 6).

Atomic Force Microscopic Studies. To obtain more insight into the supramolecular structures of the coaggregates, MCH solutions of **MPBI2·dCA** and **MPBI3·dCA** were spin-coated onto freshly cleaved highly oriented pyrolytic graphite (HOPG)

(35) A similar hypsochromically-shifted absorption band was observed for octadecylated perylene bisimide: Struijk, C. W.; Sieval, A. B.; Dakhorst, J. E. J.; van Dijk, M.; Kimkes, P.; Koehorst, R. B. M.; Donker, H.; Schaafsma, T. J.; Picken, S. J.; van de Craats, A. M.; Warman, J. M.; Zuilhof, H.; Sudholter, E. J. R. *J. Am. Chem. Soc.* **2000**, *122*, 11057–11066.

(36) Brunsveld, L.; Folmer, B. J.; Meijer, E. W.; Sijbesma, R. P. *Chem. Rev.* **2001**, *101*, 4071–4098.

(37) Lehn, J.-M. *Polym. Int.* **2002**, *51*, 825–839.

(38) Ciferri, A. *Macromol. Rapid Commun.* **2002**, *23*, 511–529.

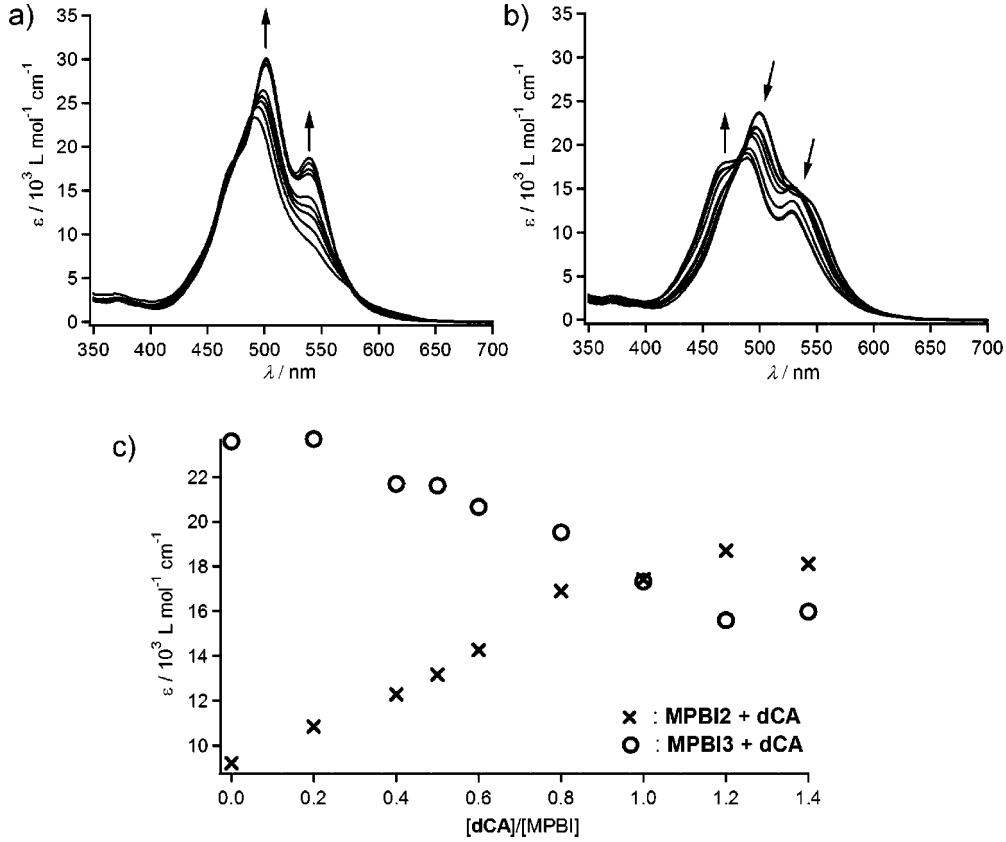

FIGURE 4. UV/vis titration of (a) **MPBI2** and (b) **MPBI3** with **dCA** at 25 °C in MCH. Concentrations of MPBIs are 1.4×10^{-5} M. (c) Plots of ϵ of **MPBI2** (×, at 540 nm) and **MPBI3** (○, at 500 nm) versus [**dCA**]/[MPBI].

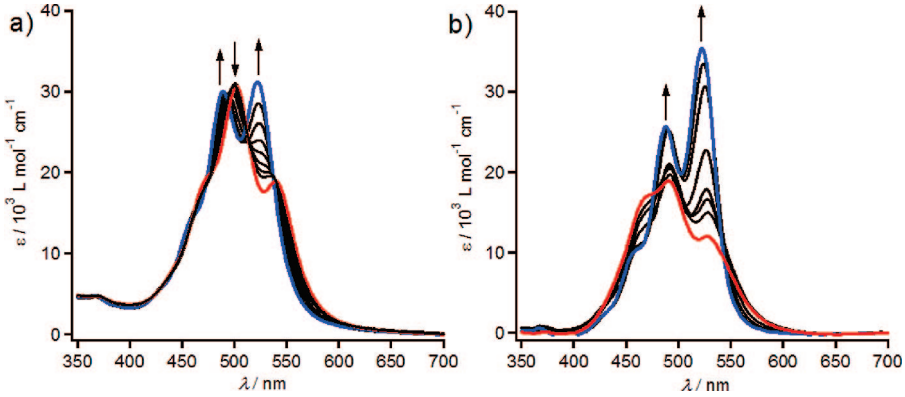

FIGURE 5. Temperature-dependent UV/vis spectra of 1:1 mixtures of (a) **MPBI2·dCA** and (b) **MPBI3·dCA** in MCH ($c = 1.4 \times 10^{-5}$ M). Temperature range: 20−90 °C. The spectra at 20 and 90 °C are drawn by red and blue lines, respectively. Arrows indicate changes upon increasing temperature.

and imaged by atomic force microscopy (AFM). For the sample prepared from freshly prepared MCH solution of **MPBI3·dCA**, ill-defined aggregates whose sizes are less than 500 nm were imaged (data not shown). This size regime is in line with that observed in the DLS analysis of the freshly prepared solution. When the sample was prepared from the solution aged for 1 h, agglomerated fibers whose sizes exceed 1 μm were imaged (Figure 8a,b). This is also in agreement with the result of the DLS. Closer inspection reveals that fibers grow from the ill-defined aggregates (circled area in Figure 8a,b). Magnified imaging displayed entangled ropelike nanostructures (Figure 8c). The thinnest ropes have widths at around 50 nm (indicated by arrow), which are entangled to form thicker ropes. These AFM images thus confirm the formation of hydrogen-bonded supramolecular polymers from **MPBI3·dCA**, which hierarchically organize into elongated ropelike nanostructures.

On the contrary, no well-defined nanostructures could be imaged for **MPBI2·dCA** even when AFM samples were prepared from aged solution (Figure 9). Only grainy surfaces were visualized, demonstrating that the discrete dimer does not organize into well-defined nanostructures in solution. However, upon evaporating the solvent slowly, a highly birefringent texture was observed by polarized optical microscopy (data not shown), showing the potential application of this discrete supramolecular species as supramolecular liquid crystalline materials.[39]

CD Studies. To further shed light on the formation of different supramolecular species from MPBIs upon mixing with

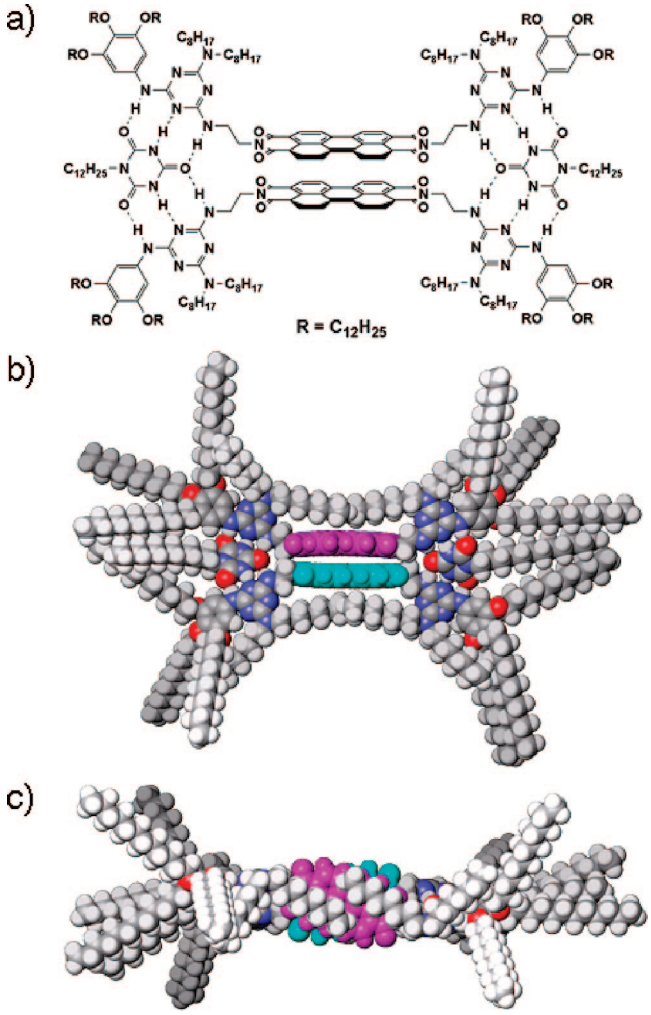

FIGURE 6. (a) Proposed supramolecular structure of discrete supramolecular species formed between **MPBI2** and **dCA**, and their molecular modeled structure viewed from (b) vertical and (c) perpendicular directions to the perylene π-plane. Perylene bisimide cores are indicated by purple and ocean blue.

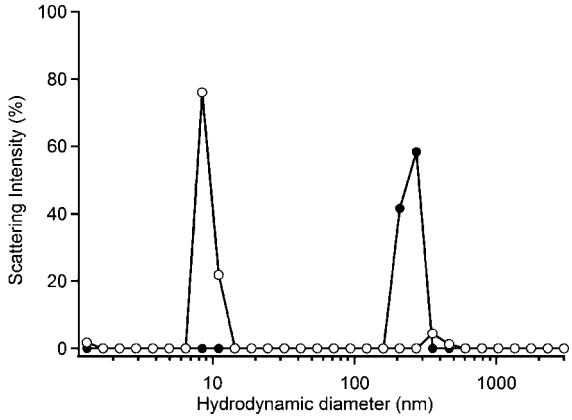

FIGURE 7. Dynamic light scattering analyses of **MPBI2·dCA** (○, $c = 1 \times 10^{-3}$ M) and **MPBI3·dCA** (●, $c = 5 \times 10^{-4}$ M) in MCH at 20 °C.

cyanurates, their aggregation with **cCA** possessing the cholesterol chiral handle was investigated by CD spectroscopy. The mixture of **MPBI2·cCA** and **MPBI3·cCA** in MCH ($c = 1.4 \times 10^{-5}$ M) shows absorption spectra almost identical to those of **MPBI2·dCA** and **MPBI3·dCA**, respectively (Figure 10a).

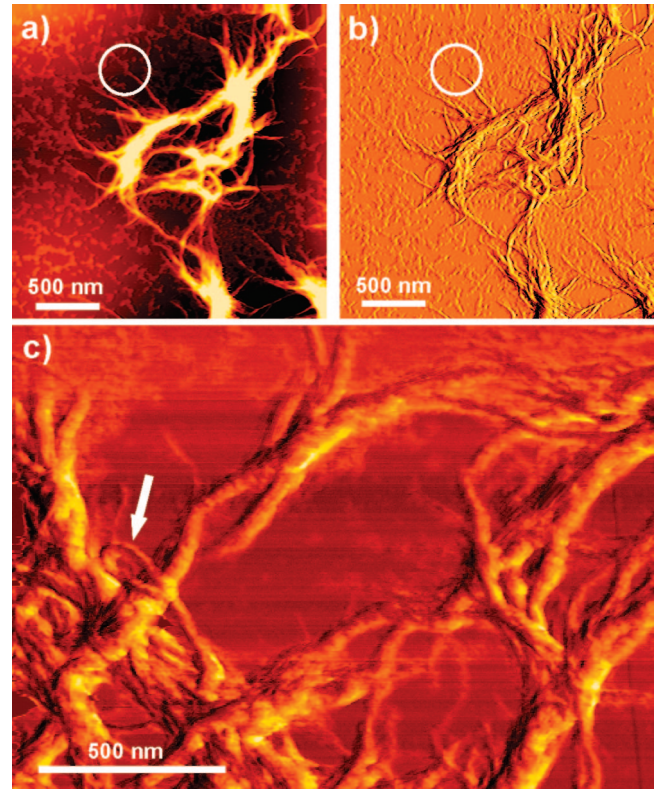

FIGURE 8. (a) AFM height (z scale = 23 nm) and (b) phase images of **MPBI3·dCA** spin-coated from MCH solution ($c = 5 \times 10^{-4}$ M). (c) Magnified image. Arrow indicates one of the thinnest ropes.

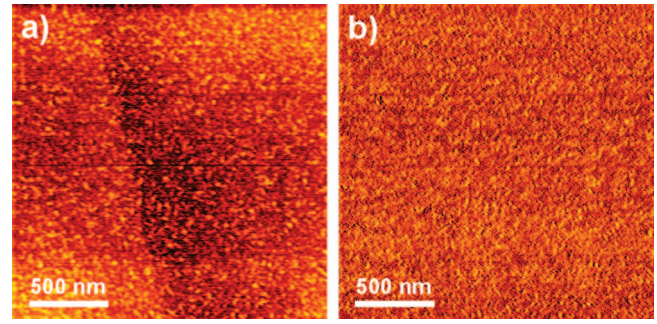

FIGURE 9. (a) AFM height (z scale = 2 nm) and (b) phase images of **MPBI2·dCA** spin-coated from MCH solution ($c = 5 \times 10^{-3}$ M).

A clear difference was observed between their CD spectra. **MPBI2·cCA** showed a positively bisignated Cotton effect with the zero-crossing point at $\lambda = 506$ nm nearly matching with the absorption maximum (Figure 10b), indicating the preferential formation of the perylene stacks with a right-handed rotational displacement.[40–43] In contrast, **MPBI3·cCA** displayed no CD signals, revealing that the perylene stacks lack a biased rotational

(39) Kato, T.; Mizoshita, N.; Kishimoto, K. *Angew. Chem., Int. Ed.* **2006**, *45*, 38–68.
(40) Nakanishi, K.; Berova, N. In *Circular Dichroism: Principles and Applications*; Woody, R., Ed.; VCH Publishers: New York, 1994; pp 361−398.
(41) Dehm, V.; Chen, Z.; Baumeister, U.; Prins, P.; Siebbeles, L. D. A.; Würthner, F. *Org. Lett.* **2007**, *9*, 1085–1088.
(42) Langhals, H.; Ismael, R. *Eur. J. Org. Chem.* **1998**, 1915–1917.
(43) Syamakumari, A.; Schenning, A. P. H. J.; Meijer, E. W. *Chem.−Eur. J.* **2002**, *8*, 3353–3361.
(44) Multiple-hydrogen-bond-directed extended aggregation and dimerization of porphyrin derivatives have been controlled by the atropisomerism of *meso*-substituents: Arai, S.; Niwa, D.; Nishide, H.; Takeoka, S. *Org. Lett.* **2007**, *9*, 17–20.

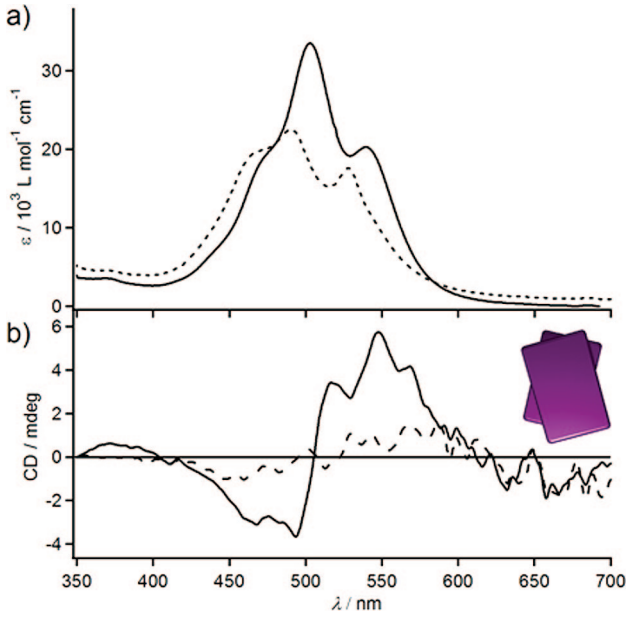

FIGURE 10. (a) UV and (b) CD spectra of 1:1 mixtures of **MPBI2·cCA** (solid curves) and **MPBI3·cCA** (dashed curves) in MCH ($c = 1.4 \times 10^{-5}$ M). Inset in (b) illustrates the orientation of two perylene cores of **MPBI2·cCA**.

displacement. The successful induction of chirality in the aggregate of **MPBI2·cCA** might be related to the formation of conformationally locked supramolecular species (Figure 6), where the peripheral chiral information can precisely be transferred to the stacking arrangement of the chromophore units. On the contrary, the aggregation of **MPBI3** with **cCA** is open-ended, so that the peripheral chiral information might fail to regulate the stacking arrangement of the chromophore units.

Discussion

As demonstrated by UV/vis studies, **MPBI2** and **MPBI3** exist as self-aggregates through $\pi-\pi$ stacking interactions between perylene cores. Temperature-dependent UV/vis measurements showed that the stabilities of these self-aggregates do not differ significantly because of the lack of specific hydrogen bonding interactions. Upon mixing with **dCA**, however, the thermal stability of the stacks of perylene cores was considerably enhanced in the case of **MPBI2** but significantly diminished in the case of **MPBI3**. This contrary effect of **dCA** is indicative of the formation of different supramolecular species, which was further supported by the successful induction of chiral stacks of perylene cores by using **cCA** as a chiral cyanurate. From the DLS and molecular modeling analyses, it is suggested that the supramolecular structure of **MPBI2·dCA** is a dimeric stack of **MPBI2** scaffolded by the two **dCA** molecules through four triple hydrogen bonds (Figure 6). Such a dimer is highly stable (the "melting" temperature at which 50% of aggregates dissociate reaches 120 °C at a concentration of 1.4×10^{-5} M) as a result of cooperative hydrogen bonding and $\pi-\pi$ stacking interactions. In contrast, **MPBI3·dCA** was shown to form hydrogen-bonded supramolecular polymers which hierarchically organize into ropelike nanostructures through $\pi-\pi$ stacking interactions. For supramolecular polymers formed between **MPBI3** and **dCA**, numerous supramolecular architectures can be drawn because of the presence of two orientations in the

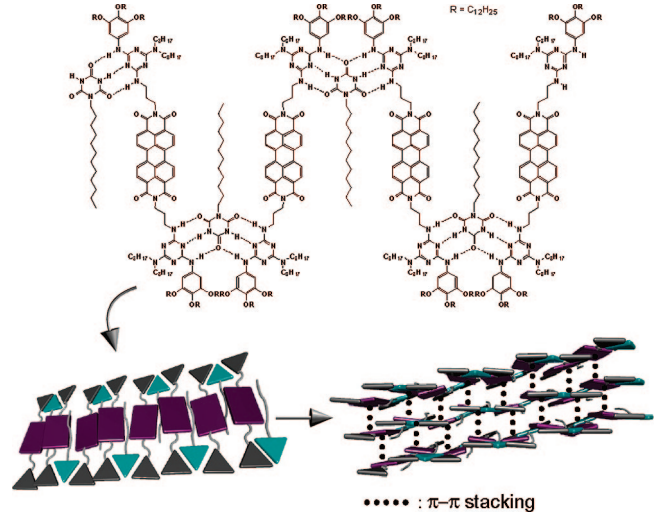

FIGURE 11. Possible local supramolecular structure for hydrogen-bonded supramolecular polymers of **MPBI3·dCA** and the schematic presentation of their hierarchical organization through multipoint $\pi-\pi$ stacking interactions.

donor−acceptor−donor•acceptor−donor−acceptor triple hydrogen bonds between melamines and cyanurates. However, by taking into account the formation of well-defined ropelike nanostructures, their supramolecular architectures should be uniform between supramolecules, and the orientation of triple hydrogen bonds should be regular within a supramolecular polymer. A possible supramolecular architecture is shown in Figure 11, which nicely illustrates the lower thermal stability of the stacks of perylene cores in **MPBI3·dCA** than in **MPBI2·dCA**. In this structure, perylene cores cannot approach within a hydrogen-bonded supramolecular chain due to the presence of dodecyl chains of **dCA**, so that $\pi-\pi$ stacking may occur only between supramolecular polymers.

Conclusions

We have demonstrated that the two distinct supramolecular species of perylene bisimide, i.e., supramolecular polymer and discrete dimer, can be constructed by mixing melamine-appended perylene bisimides (MPBIs) and cyanurates.[44] The supramolecular architectures are determined by the number of carbon atoms at the linker moieties of MPBIs. Supramolecular polymers are formed when the number of carbon atoms is three, which hierarchically organize into nanosized ropes. Such phase-separated quasi-one-dimensional nanoobjects have potential applications in optically and electronically active nanomaterials. On the other hand, a discrete dimer can be constructed when the number of carbon atom is two. Such a discrete supramolecular species is highly soluble even in nonpolar organic solvents and thus is applicable to a processable supramolecular element for the fabrication of organic bulk materials exhibiting unique optical and electronic properties distinct from those of monomeric chromophores or extended one-dimensional stacks of chromophores. Thus, a variety of supramolecular functional materials might be produced from melamine-linked functional dyes through the complexation with cyanurates.

Experimental Section

MPBI2 and **MPBI3** were prepared according to Scheme 1. The synthesis of **cCA** will be reported elsewhere. 3,4,5-Tri(dodecyloxy)aniline was prepared according to a literature method.[45]

2-Chloro-4-dioctylamino-6-{(3,4,5-tridodecyloxyphenyl)amino}-[1,3,5]triazine (4): 442 mg of 3,4,5-tri(dodecyloxy)aniline (0.684 mmol) in 10 mL of dry THF was added to a dry THF solution (50 mL) of 126 mg of 1,3,5-trichloro-*s*-triazine (0.689 mmol) and 2.0 mL of diisopropylethylamine (DIPEA) at room temperature, and the mixture was stirred for 2 h. Additional DIPEA (1.5 mL) and 170 mg of dioctylamine (0.705 mmol) were added dropwise. After stirring for 2.5 h at room temperature, solvent was evaporated, and the residue was dissolved in an appropriate amount of $CHCl_3$. The resulting solution was washed with 2 M hydrochloric acid and then water, and the separated organic phase was dried over Na_2SO_4. After the solvent was evaporated, the residue was purified by silica gel column chromatography (10% AcOEt in hexane) to give **4** (490 mg, 71% yield): ^{1}H NMR (400 MHz, $CDCl_3$) δ = 6.75 (s, 2H), 3.95 (m, 6H), 3.52 (m, 4H), 1.80 (m, 4H), 1.30 (m, 80H), 0.88 (t, 15H).

2-(2-Aminoethyl)-4-dioctylamino-6-{(3,4,5-tridodecyloxyphenyl)amino}-[1,3,5]triazine (1): A dry THF solution of compound **4** (450 mg) and 10 equiv of 1,2-diaminoethane was refluxed overnight under a nitrogen atmosphere. After cooling to room temperature, the mixture was filtered to remove the resulting precipitates. The filtrate was evaporated, and the residue was redissolved in $CHCl_3$. The resulting solution was washed with 2 M hydrochloric acid and then water, and the separated organic phase was dried over Na_2SO_4. After the solvent was evaporated, the residue was purified by silica gel column chromatography (10% MeOH in $CHCl_3$ as an eluent) to give compound **1** (338 mg, 73% yield): ^{1}H NMR (400 MHz, $CDCl_3$) δ = 6.86 (s, 2H), 3.86 (m, 6H), 3.77 (m, 2H), 3.51 (m, 2H), 3.40 (m, 2H), 3.30 (m, 2H), 1.72 (m, 6H), 1.53 (m, 4H), 1.38−1.22 (m, 74H), 0.88 (t, 15H).

2-(3-Aminopropyl)-4-dioctylamino-6-{(3,4,5-tridodecyloxyphenyl)amino}-[1,3,5]triazine (2): This compound was prepared from 400 mg of **4** and 10 equiv of 1,3-diaminopropane in the same way as described for **1** (yield 290 mg (70%)): ^{1}H NMR (400 MHz, $CDCl_3$) δ = 6.88 (s, 2H), 3.91 (m, 6H), 3.60 (m, 2H), 3.50 (m, 4H), 3.11 (m, 2H), 2.07 (m, 2H), 1.72 (m, 6H), 1.59 (m, 4H), 1.30 (m, 74H), 0.88 (t, 15H).

***N,N′*-Bis[2-{4-dioctylamino-6-(3,4,5-tris-dodecyloxy-phenyl)-amino-[1,3,5]triazin-2-ylamino}-ethyl]perylene-3,4:9,10-tetracarboxylic Acid Bisimide (MPBI2):** Perylene-3,4:9,10-tetracarboxylic acid bisanhydride (44 mg, 0.11 mmol), compound **1** (338 mg, 0.330 mmol), zinc acetate (50 mg), and imidazole (3.1 g) were refluxed under nitrogen overnight. After cooling to room temperature, the mixture was dissolved in $CHCl_3$ and washed with 2 M hydrochloric acid and then water. The organic layer was separated and subsequently dried over Na_2SO_4 and concentrated under vacuum. Purification of the residue by silica gel column chromatography (2.5% MeOH in $CHCl_3$ as an eluent) and reprecipitation from the MeOH−$CHCl_3$ mixture gave **MPBI2** as a red solid (183 mg, 68% yield): ^{1}H NMR (500 MHz, 1,1,2,2-tetrachloroethane-d_2, 90 °C) δ = 8.54 (m, J = 8.0 Hz, 4H), 8.42 (m, J = 8.0 Hz, 4H), 6.68 (s, 4H), 4.43 (m, J = 6.5 Hz, 4H), 3.83 (m, 16H), 3.42 (m, 8H), 1.64 (m, 20H), 1.28 (m, 148H), 0.85 (t, 30H); ^{13}C NMR (125 MHz, 1,1,2,2-tetrachloroethane-d_2, 90 °C) δ = 164.8, 154.4, 135.9, 132.7, 130.7, 127.8, 124.5, 124.4, 101.8, 70.9, 48.6, 44.8, 41.5, 413, 33.2, 33.1, 31.7, 31.0, 30.9, 30.8, 30.6, 30.5, 29.3, 28.3, 27.5, 23.9, 15.3. MS (MALDI-TOF) calcd for $C_{150}H_{242}N_{14}O_{10}Na$ (m/z) 2424.6 [M + Na]$^+$, found 2423.9. Anal. Calcd for $C_{150}H_{242}N_{14}O_{10}\cdot 2H_2O$: C, 73.91; H, 10.17; N, 8.04. Found: C, 73.94; H, 10.16; N, 8.09.

***N,N′*-Bis[3-{4-dioctylamino-6-(3,4,5-tris-dodecyloxy-phenyl)-amino-[1,3,5]triazin-2-ylamino}-propyl]perylene-3,4:9,10-tetracarboxylic Acid Bisimide (MPBI3):** Perylene-3,4:9,10-tetracarboxylic acid bisanhydride (40 mg, 0.10 mmol), compound **2** (290 mg, 0.280 mmol), zinc acetate (39 mg), and imidazole (3.1 g) were refluxed under nitrogen for 7 h. After cooling to room temperature, the mixture was dissolved in $CHCl_3$ and washed with 2 M hydrochloric acid and then water. The organic layer was separated and subsequently dried over Na_2SO_4 and concentrated under vacuum. Purification of the residue by silica gel column chromatography (3% MeOH in $CHCl_3$) and reprecipitation from the $CHCl_3$−MeOH mixture gave **MPBI3** as a red solid (132 mg, 53% yield): ^{1}H NMR (500 MHz, 1,1,2,2-tetrachloroethane-d_2, 90 °C) δ = 8.63 (m, J = 8.0 Hz, 4H), 8.53 (m, J = 8.0 Hz, 4H), 6.76 (s, 4H), 4.29 (t, J = 6.5 Hz, 4H), 3.87 (m, 16H), 3.48 (m, 8H), 2.08 (m, 4H), 1.80 (m, 20H), 1.30 (m, 148H), 0.85 (t, 30H); ^{13}C NMR (125 MHz, 1,1,2,2-tetrachloroethane-d_2, 90 °C) δ = 162.9, 152.6, 134.2, 130.9, 128.9, 126.0 122.7, 122.6, 101.5, 69.0, 47.0, 43.9, 42.0, 41.8, 38.0, 31.2, 31.1, 29.8, 29.1, 29.0, 28.8, 28.6, 28.5, 27.4, 26.4, 25.6, 21.9, 13.4. MS (MALDI-TOF) calcd for $C_{152}H_{246}N_{14}O_{10}$ (m/z) 2429.7 [M$^+$], found 2430.0. Anal. Calcd for $C_{152}H_{246}N_{14}O_{10}\cdot 3H_2O$: C, 73.50; H, 10.23; N, 7.90. Found: C, 73.21; H, 10.34; N, 7.86.

Acknowledgment. We thank Ms. Kanako Unoike of Chiba University for the measurement of AFM and Dr. Yasuo Norikane and Dr. Nobuyuki Tamaoki of National Institute of Advanced Industrial Science and Technology (AIST, Tsukuba, Japan) for MALDI-TOF MS measurement.

Supporting Information Available: Materials and methods and ^{1}H and ^{13}C NMR spectra of **MPBI2** and **MPBI3**. This material is available free of charge via the Internet at http://pubs.acs.org.

JO800338F

(45) Percec, V.; Ahn, C.-H.; Bera, T. K.; Ungar, G.; Yeardley, D. J. P. *Chem.−Eur. J.* **1999**, *5*, 1070–1083.